Sensor and Actuator Placement for Proportional Feedback Control in Advection-Diffusion Equations

D. W. M. Veldman, R. H. B. Fey, H. J. Zwart, *Member, IEEE*, M. M. J. van de Wal, J. D. B. J. van den Boom, and H. Nijmeijer, *Fellow, IEEE*

***Abstract*—In this letter, advection-diffusion equations with constant coefficients on infinite 1-D and 2-D spatial domains are considered. Suitable sensor and/or actuator locations are determined for which high-gain and low-gain proportional feedback can effectively reduce the influence of a disturbance at a point of interest. These locations are characterized by simple analytic expressions which can be used as guidelines for control system design. The obtained analytic expressions are validated by numerical results.**

***Index Terms*—Distributed parameter systems, control system architecture, PID control.**

I. Introduction

THE PLACEMENT of sensors and actuators is an important aspect of control system design for which many techniques have been developed (see, e.g., [1]). The simplest approach to this problem is to choose a controller design method and evaluate the resulting closed-loop performance for a large number of sensor and/or actuator locations. However, such an approach is computationally demanding when there are a large number of potential sensor and/or actuator locations. This is typically the case when the problem is governed by Partial Differential Equations (PDEs).

Several publications have considered the sensor and/or actuator placement problem for parabolic PDEs such as the heat equation. For example, Burns and Rubio [2] proposed a strategy for sensor placement based on the kernel representation of feedback operators in infinite-dimensional linear quadratic estimation problems. More recent results can be found in [3], [4]. Another approach proposed by Armaou and Demetriou [5] used modal observability and controllability measures to determine optimal sensor and actuator locations in parabolic PDEs. In the approach proposed by Vaidya *et al.* [6] the optimal area for sensing or actuation in advective PDEs is determined by maximizing the support of the observability or controllability Gramian, respectively. The idea to determine the optimal area for sensing was also considered by Privat *et al.* [7], who proposed a method to determine the optimal area for sensing by minimizing a randomized observability constant. A similar idea can be used to determine the optimal area for actuation [8].

These approaches do not explicitly address the design of the resulting feedback controller (and/or observer). This is an important aspect of the control system design which may affect the found optimal sensor and actuator locations. Such combined actuator location and controller optimization problems have been considered in [9], [10], [11], [12]. The dual problem in which the variance of the estimation error is minimized over sensor locations and observers has also been addressed in [3], [4], [13]. An additional problem is that practical implementation requires that the order of the controller (and/or observer) is sufficiently low. This seems to be a largely open problem, for which some potential solutions have been proposed by Demetriou [14], [15].

In many of the approaches that address the design of a feedback controller (and/or observer), the optimal sensor and/or actuator locations by searching through a discrete set of potential sensor and/or actuation locations, see, e.g., [10], [13], [14]. Such an approach does not seem to use the connection to the underlying PDE fully.

In this letter, the placement of a single sensor and/or a single actuator in advection-diffusion equations with proportional feedback control is addressed. The problem is considered on one- and two-dimensional infinite spatial domains. Based on analytic expressions for the transfer functions, geometric rules that characterize the optimal sensor and actuator locations

Manuscript received March 1, 2019; revised May 2, 2019; accepted May 25, 2019. Date of publication June 7, 2019; date of current version June 24, 2019. Recommended by Senior Editor C. Prieur. *(Corresponding author: D. W. M. Veldman.)*

D. W. M. Veldman, R. H. B. Fey, and H. Nijmeijer are with the Department of Mechanical Engineering, Eindhoven University of Technology, 5600 MB Eindhoven, The Netherlands (e-mail: d.w.m.veldman@tue.nl; r.h.b.fey@tue.nl; h.nijmeijer@tue.nl).

H. J. Zwart is with the Department of Mechanical Engineering, Eindhoven University of Technology, 5600 MB Eindhoven, The Netherlands, and also with the Department of Applied Mathematics, Faculty of Electrical Engineering, Mathematics, and Computer Science, University of Twente, 7500 AE, Enschede, The Netherlands (e-mail: h.j.zwart@tue.nl).

M. M. J. van de Wal is with Research, ASML, 5504 DR Veldhoven, The Netherlands (e-mail: marc.van.de.wal@asml.com).

J. D. B. J. van den Boom is with the Development and Engineering, ASML, 5504 DR Veldhoven, The Netherlands (e-mail: joris.van.den.boom@asml.com).

Digital Object Identifier 10.1109/LCSYS.2019.2921623

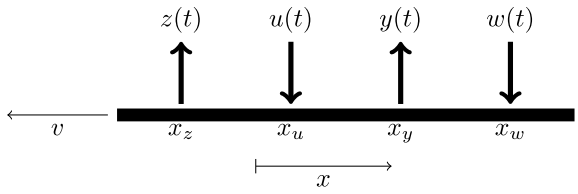

Fig. 1. The 1-D spatial domain with the locations of the sensor, actuator, disturbance, and performance variable.

for high-gain and low-gain feedback are derived. Numerical experiments indicate that the derived rules accurately predict all (locally) optimal actuator and/or sensor locations.

The remainder of this letter is structured as follows. In Section II, the analysis and numerical results for the one-dimensional spatial domain are presented. In Section III, the two-dimensional spatial domain is considered. In Section IV, the conclusions are formulated and future work is discussed.

II. One-Dimensional Spatial Domain

Consider the following PDE with constant coefficients on the one-dimensional spatial domain $x \in \mathbb{R}$

$$\frac{\partial T}{\partial t} = v\frac{\partial T}{\partial x} + D\frac{\partial^2 T}{\partial x^2} - hT + \frac{1}{c}\delta(x-x_u)u(t) + \frac{1}{c}\delta(x-x_w)w(t), \quad (1)$$

$$y(t) = T(x_y,t), \qquad z(t) = T(x_z,t), \quad (2)$$

with initial condition $T(x,0) = 0$. Here, $\delta(x)$ denotes the Dirac delta. This PDE can be used to model the temperature $T = T(x,t)$ [K] in a medium with heat capacity $c > 0$ [J/K/m], thermal diffusivity $D > 0$ [m^2/s], cooling rate to the environment $h > 0$ [1/s], and advective transport with velocity $v \geq 0$ [m/s].

The problem is to find the locations x_u [m] of the control input $u(t)$ [W] and x_y [m] of the measured output $y(t)$ [K] for which there exists a proportional feedback controller that minimizes the influence of the disturbance $w(t)$ [W] entering at $x = x_w$ [m] on the performance variable $z(t)$ [K] at $x = x_z$ [m]. The considered situation is illustrated in Fig. 1.

The transfer function of this system can be found by transforming (1)–(2) to the Laplace domain and solving the resulting ODE in x for the Laplace transform of T (see, e.g., [16] for a more elaborate discussion). This yields

$$\begin{bmatrix} Z(s) \\ Y(s) \end{bmatrix} = \begin{bmatrix} G_{zw}(s) & G_{zu}(s) \\ G_{yw}(s) & G_{yu}(s) \end{bmatrix} \begin{bmatrix} W(s) \\ U(s) \end{bmatrix} = \begin{bmatrix} G(s, x_z - x_w) & G(s, x_z - x_u) \\ G(s, x_y - x_w) & G(s, x_y - x_u) \end{bmatrix} \begin{bmatrix} W(s) \\ U(s) \end{bmatrix}, \quad (3)$$

where $Z(s)$, $Y(s)$, $W(s)$, and $U(s)$ denote the Laplace transforms of $z(t)$, $y(t)$, $w(t)$, and $u(t)$, respectively, and

$$G(s,x) = \frac{1}{c}\frac{e^{-xv/2D}}{\sqrt{v^2+4D(s+h)}}e^{-|x|\sqrt{v^2+4D(s+h)}/2D}. \quad (4)$$

Remark 1: The $\mathcal{H}_\infty$-norm of $G(s,x)$ is bounded by

$$\|G(\cdot,x)\|_\infty = G(0,x) \leq \frac{e^{-(xv+|xv|)/2D}}{c\sqrt{v^2+4Dh}}. \quad (5)$$

Therefore, the advection dominated control problem (i.e., $|v(x_z - x_w)| \gg 2D$) is only relevant when x_z lies downstream of x_w (i.e., $(x_z - x_w)v < 0$). Otherwise, the bound on the $\mathcal{H}_\infty$-norm in (5) shows that $\|G_{zw}\|_\infty \approx 0$ and control is not necessary.

Under proportional control $u(t) = -Py(t)$, the closed loop transfer function from $W(s)$ to $Z(s)$ is given by

$$M(s) := G_{zw}(s) - \frac{G_{zu}(s)PG_{yw}(s)}{1+PG_{yu}(s)}. \quad (6)$$

The objective is to a find a sensor location x_y and/or an actuator location x_u for which there exists a (stabilizing) feedback gain P that makes $\|M\|_\infty$ as small as possible.

Note that for high-gain feedback ($|PG_{yu}(s)| \gg 1$)

$$M(s) \approx M_{\mathrm{HG}}(s) := G_{zw}(s) - \frac{G_{zu}(s)G_{yw}(s)}{G_{yu}(s)}, \quad (7)$$

and that for low-gain feedback ($|PG_{yu}(s)| \ll 1$)

$$M(s) \approx M_{\mathrm{LG}}(s) := G_{zw}(s) - G_{zu}(s)PG_{yw}(s). \quad (8)$$

The following two lemmas describe which choices of sensor and actuator locations make $M_{\mathrm{HG}}(s)$ and $M_{\mathrm{LG}}(s)$ small.

Lemma 1: Consider the transfer functions in (3)–(4). The high-gain feedback approximation $M_{\mathrm{HG}}(s)$ in (7) is zero for all s precisely when

$$|x_z - x_u| + |x_y - x_w| = |x_y - x_u| + |x_z - x_w|. \quad (9)$$

Proof: Using (3)–(4), the second term on the RHS of (7) can be rewritten as

$$\frac{G_{zu}(s)G_{yw}(s)}{G_{yu}(s)} = \frac{1}{c}\frac{e^{-(x_z-x_w)v/2D}}{\sqrt{v^2+4D(s+h)}} \times e^{-(|x_z-x_u|+|x_y-x_w|-|x_y-x_u|)\sqrt{v^2+4D(s+h)}/2D}. \quad (10)$$

To obtain $M_{\mathrm{HG}}(s) \equiv 0$, this expression should be equal to $G_{zw}(s)$. This is the case when the second exponential factor in (10) is equal to the second exponential factor of $G_{zw}(s)$. These are equal precisely when (9) holds. ∎

It is not possible to achieve $M_{\mathrm{LG}}(s) = 0$ for all s. Since the magnitude of $G(i\omega,x)$ is maximal for $\omega = 0$ (see also Remark 1), it is most important to make $M_{\mathrm{LG}}(s)$ small near $s = 0$. Locations where this is the case are characterized by the following result. Here, $'$ denotes the derivative w.r.t. s.

Lemma 2: Consider the transfer functions in (3)–(4). There exists a $P > 0$ such that $M_{\mathrm{LG}}(s)$ in (8) satisfies $M_{\mathrm{LG}}(0) = M'_{\mathrm{LG}}(0) = 0$ precisely when

$$|x_z - x_u| + |x_y - x_w| = |x_z - x_w| - \frac{2D}{\sqrt{v^2+4Dh}}. \quad (11)$$

Proof: Since $G(0,x)$ in (4) is positive, it is clear that

$$P = G_{zw}(0)/(G_{zu}(0)G_{yw}(0)), \quad (12)$$

is positive and that this choice for P makes $M_{\mathrm{LG}}(0)$ in (8) zero. To compute $M'_{\mathrm{LG}}(0)$, note that

$$G'(s,x) = -\left(\frac{2D}{\sqrt{v^2+4D(h+s)}} + |x|\right)\frac{G(s,x)}{\sqrt{v^2+4D(h+s)}}. \quad (13)$$

Using (8) and the choice of P in (12) it now follows that

$$\begin{aligned} M'_{\mathrm{LG}}(0) &= G'_{zw}(0) - G'_{zu}(0)PG_{yw}(0) - G_{zu}(0)PG'_{yw}(0) \\ &= G'_{zw}(0) - G_{zw}(0)\left(\frac{G'_{zu}(0)}{G_{zu}(0)} + \frac{G'_{yw}(0)}{G_{yw}(0)}\right) \\ &= \frac{G_{zw}(0)}{\sqrt{v^2+4Dh}}\left(\frac{2D}{\sqrt{v^2+4Dh}} + |x_z - x_u| \right. \\ &\qquad \left. + |x_y - x_w| - |x_z - x_w|\right). \end{aligned} \tag{14}$$

This expression is zero precisely when (11) holds. ■

It is important to note that Lemma 1 and 2 consider approximations of the closed-loop transfer function $M(s)$ based on the assumption that $|PG_{yu}(s)| \gg 1$ or $|PG_{yu}(s)| \ll 1$, respectively. Whether these assumptions can be realized is not obvious. In particular, the high-gain feedback assumption $|PG_{yu}(s)| \gg 1$ typically leads to instability and it is not clear that the P selected in Lemma 2 indeed satisfies the low-gain assumption $|PG_{yu}(s)| \ll 1$.

The following result demonstrates that the high-gain feedback assumption can be achieved for a particular sensor and actuator placement.

Corollary 1: Consider (1)–(2) and let x_z, x_w be fixed. If $x_y = x_u$, the proportional feedback controller $u(t) = -Py(t)$ is stabilizing for all $P > 0$. Furthermore, if $x_y = x_u$ is chosen between x_z and x_w there exists a $P > 0$ such that $\|M\|_\infty < \varepsilon$ for any $\varepsilon > 0$.

Proof: Consider (1)–(2) with $w(t) = 0$ and $x_y = x_u$. Then the Lyapunov function $V(t) = \int_{-\infty}^{+\infty} T^2(x,t)\,\mathrm{d}x$ has time derivative $\dot{V}(t) = u(t)y(t) = -Py^2(t)$. This implies that the closed loop is stable for all $P > 0$. Now note that for $P \to \infty$, $M(s) \to M_{\mathrm{HG}}(s)$ and that Lemma 1 asserts that $M_{\mathrm{HG}}(s) \equiv 0$ if (9) holds. For $x_y = x_u$, (9) reduces to $|x_z - x_u| + |x_u - x_w| = |x_z - x_w|$. This equation is satisfied when x_u is between x_z and x_w. ■

Remark 2: Similarly as in [17], it can be shown that if all stabilizing (dynamic) controllers are considered $\|M\|_\infty$ can be made arbitrarily small for all choices of x_y and x_u.

Remark 3: When $x_y \neq x_u$, the feedback $u(t) = -Py(t)$ will always be destabilizing for P sufficiently large.

Remark 4: Note that the result in Corollary 1 applies to any x_w and x_z chosen on opposite sides of $x_y = x_u$. A consequence of Corollary 1 is therefore that when the area in which the disturbance(s) are applied lies on the opposite side of $x_y = x_u$ as the area in which the performance variable(s) are measured, the influence of the disturbances on the performance variables can be made arbitrarily small by a stabilizing proportional feedback controller.

Corollary 1 addresses a particularly effective sensor and actuator placement, which might not always be possible to achieve. Therefore, it is now assumed that the location of the actuator x_u is already fixed, i.e., for given x_z, x_w, and x_u, the goal is to find the optimal x_y for high-gain and low-gain proportional feedback control.

The optimal choice of x_y for high-gain proportional feedback depends on the ordering of x_z, x_w, and x_u. If x_u is between x_z and x_w, Corollary 1 shows that the optimal choice for x_y is $x_y = x_u$. If x_z is between x_u and x_w, it can be verified that (9) only holds when $x_y = x_z$. If x_w is between x_z and x_u, it can be shown that (9) holds for all x_y that are on the same side of x_w as x_z. Because a greater distance $|x_y - x_u|$ limits the range of stabilizing gains P, the optimal choice for x_y is $x_y = x_w$ in this case.

The optimal choice of x_y for low-gain proportional feedback control follows from (11), which typically gives two potential choices of x_y at equal distance of x_w. Note however that if $|x_z - x_w| < |x_z - x_u|$, (11) cannot be satisfied for any x_y. Furthermore, these potential optimal locations are only good choices if the low-gain feedback assumption $|PG_{yu}(s)| \ll 1$ is satisfied at these locations. To check this, note that for the value of P in (12), $\|PG_{yu}\|_\infty$ is equal to

$$e^{(|x_z-x_u|+|x_y-x_w|-|x_z-x_w|-|x_y-x_u|)\sqrt{v^2+4Dh}/2D}. \tag{15}$$

For each of the two potential low-gain feedback locations, it should be checked whether this number is small.

The method to determine the optimal sensor locations is validated by designing the optimal proportional feedback controller for a range of sensor locations x_y while keeping the locations x_z, x_w, x_u fixed. The controller was designed as follows. First, the transfer function $G_{yw}(s)$ is evaluated on a grid of 4,000 frequency points $s = i\omega_k$ logarithmically distributed between $2\pi \cdot 10^{-2}$ and $2\pi \cdot 10^{6}$. The maximal allowable gain $P_{\max}$ for which the modulus margin is 0.5 is found by solving $\min_k |1+PG_{yu}(i\omega_k)| = 0.5$ with `fzero` in MATLAB (version R2017b). The optimal gain P is determined by minimizing $\max_k |M(i\omega_k)|$ over $P \in [0, P_{\max}]$ using `fminbnd`.

Fig. 2 shows the closed-loop performance $\|M\|_\infty$ that can be obtained for the controller designed at each of the sensor locations. Note that $\|M\|_\infty$ is normalized w.r.t. open loop performance $\|G_{zw}\|_\infty$. The used parameter values are $c = 33$ [J/K/m], $v = 0$ [m/s], $D = 91 \cdot 10^{-6}$ [m^2/s], and $h = 1$ [1/s]. These are based on a previous wafer heating case study in [18]. The locations x_z, x_w, and x_u are chosen rather arbitrary. The red arrows indicate the predicted optimal locations for high-gain feedback, the green arrows indicate the predicted locations for low-gain feedback. A green dashed arrow indicates that (15) is larger than 0.1, i.e., that the low-gain feedback assumption is not satisfied. The three subfigures represent the three possible orderings of x_z, x_w, and x_u. The locations of the observed local minima are all very close to the predicted optimal locations. Note that Fig. 2(c) represents the situation where $|x_z - x_w| < |x_z - x_u|$ for which (11) does not provide potential optimal locations for low-gain feedback.

Fig. 3 represents the advection-dominated case where v is set to 0.33 [m/s] and the other parameters are the same as in Fig. 2. Again a very good match is obtained between the observed local minima and the potential optimal sensor locations. It is important to note that the characteristic length $2D/v = 0.55$ mm is very small in this situation. Remark 1 thus shows that only situations where $x_z \leq x_w$ are of interest because $\|G_{zw}\|_\infty$ is negligible otherwise. Similar reasoning shows that $\|G_{zu}\|_\infty$ is negligible when $x_u < x_z < x_w$, which means that $z(t)$ cannot be affected by the control input. This situation is therefore not of interest. The two remaining

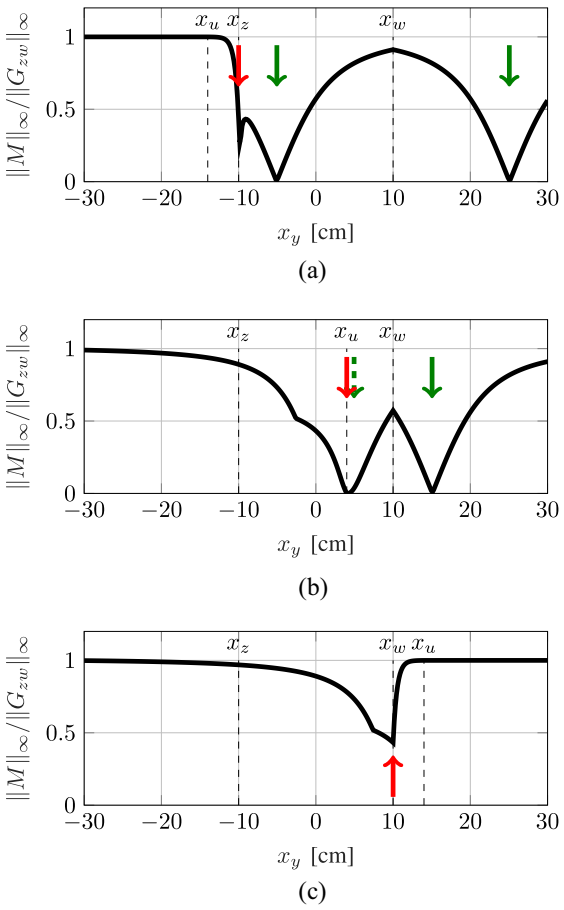

Fig. 2. Closed-loop performance $\|M\|_\infty$ for varying sensor location x_y in the diffusion-dominated problem (the red arrows indicate locations where (9) is satisfied and the green arrows indicate locations where (11) is satisfied). (a) $x_u = -14$ cm, $x_z = -10$ cm, $x_w = 10$ cm. (b) $x_z = -10$ cm, $x_u = 4$ cm, $x_w = 10$ cm. (c) $x_z = -10$ cm, $x_w = 10$ cm, $x_u = 14$ cm.

orderings of x_z, x_w, and x_u are considered in the Fig. 3. Locations where $x_y > x_w$ are indicated by black dotted lines, because $\|G_{yw}\|_\infty$ is negligible there.

Fig. 4 demonstrates that similar techniques can be used to determine the optimal actuator location x_u for a fixed sensor location x_y. The parameter values in Fig. 4 are the same as in Fig. 3. The figure clearly indicates that the roles of (x_y, x_u) and (x_z, x_w) are interchanged.

III. Two-Dimensional Spatial Domain

Now consider the following parabolic PDE with constant coefficients on $\mathbf{x} = (x_1, x_2) \in \mathbb{R}^2$

$$\frac{\partial T}{\partial t} = v\frac{\partial T}{\partial x_1} + D\frac{\partial^2 T}{\partial x_1^2} + D\frac{\partial^2 T}{\partial x_2^2} - hT + \frac{1}{c_2}\delta(\mathbf{x} - \mathbf{x}_u)u(t) + \frac{1}{c_2}\delta(\mathbf{x} - \mathbf{x}_w)w(t), \quad (16)$$

$$y(t) = T(\mathbf{x}_y, t), \qquad z(t) = T(\mathbf{x}_z, t), \quad (17)$$

with initial condition $T(x_1, x_2, 0) = 0$. Here, $\delta(x)$ denotes the Dirac delta. Similarly as before, this PDE can be used to model the temperature field $T = T(x_1, x_2, t)$ [K] in a medium with heat capacity c_2 [J/K/m^2], thermal diffusivity D [m^2/s],

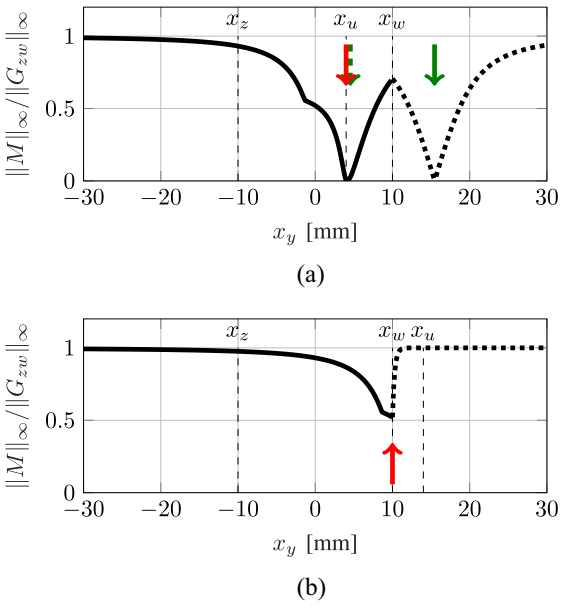

Fig. 3. Closed-loop performance $\|M\|_\infty$ for varying sensor location x_y in the advection-dominated problem (the red arrows indicate locations where (9) is satisfied and the green arrows indicate locations where (11) is satisfied). (a) $x_z = -10$ mm, $x_u = 4$ mm, $x_w = 10$ mm. (b) $x_z = -10$ mm, $x_w = 10$ mm, $x_u = 14$ mm.

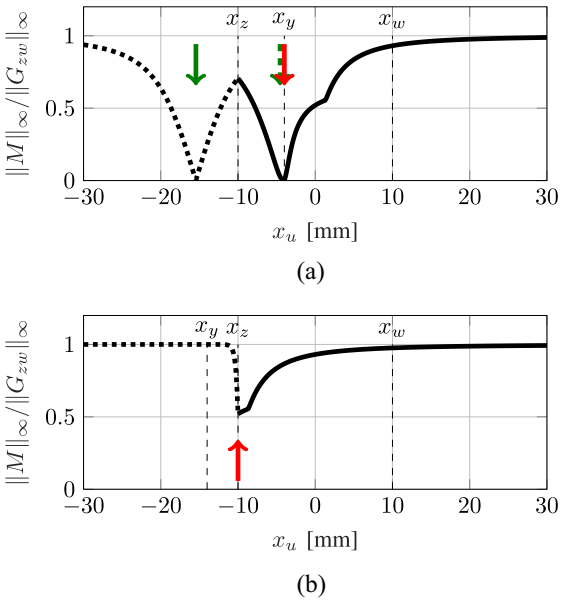

Fig. 4. Closed-loop performance $\|M\|_\infty$ for varying actuator location x_u in the advection-dominated problem (the red arrows indicate locations where (9) is satisfied and the green arrows indicate locations where (11) is satisfied). (a) $x_z = -10$ mm, $x_y = -4$ mm, $x_w = 10$ mm. (b) $x_y = -14$ mm, $x_z = -10$ mm, $x_w = 10$ mm.

cooling rate h [1/s], and advective transport with velocity $v \geq 0$ [m/s]. Without loss of generality, it can be assumed that the velocity is in the x_1-direction. The input and output locations $\mathbf{x}_u = (x_{1,u}, x_{2,u})$, $\mathbf{x}_w = (x_{1,w}, x_{2,w})$, $\mathbf{x}_y = (x_{1,y}, x_{2,y})$, and $\mathbf{x}_z = (x_{1,z}, x_{2,z})$ now consist of two components. The considered situation is shown in Fig. 5.

Following the method described in [16], it follows that finding the transfer function of (16)–(17) requires the solution of an elliptic PDE in two spatial dimensions which has the

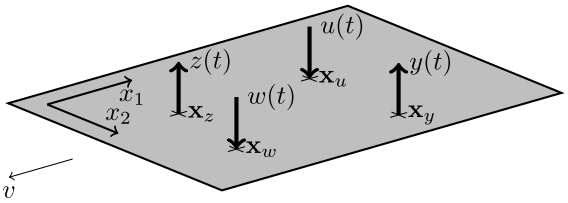

Fig. 5. The 2-D spatial domain with the locations of the sensor, actuator, disturbance, and performance variable.

closed-form solution derived in [19, Ch. 11.3]. The relations between inputs and outputs can now be written in the Laplace domain as

$$\begin{bmatrix} Z(s) \\ Y(s) \end{bmatrix} = \begin{bmatrix} G_{zw}(s) & G_{zu}(s) \\ G_{yw}(s) & G_{yu}(s) \end{bmatrix} \begin{bmatrix} W(s) \\ U(s) \end{bmatrix} = \begin{bmatrix} G(s, \mathbf{x}_z - \mathbf{x}_w) & G(s, \mathbf{x}_z - \mathbf{x}_u) \\ G(s, \mathbf{x}_y - \mathbf{x}_w) & G(s, \mathbf{x}_y - \mathbf{x}_u) \end{bmatrix} \begin{bmatrix} W(s) \\ U(s) \end{bmatrix}, \quad (18)$$

with

$$G(s, \mathbf{x}) = \frac{e^{-x_1 v/2D}}{2\pi c_2 D} K_0\Big(\sqrt{v^2 + 4D(h+s)}\|\mathbf{x}\|/(2D)\Big), \quad (19)$$

where $K_0(\zeta)$ denotes the modified Bessel function of the second kind of order 0 and $\|\mathbf{x}\| := \sqrt{x_1^2 + x_2^2}$ is the Euclidean norm.

Similarly as on the one-dimensional spatial domain, conditions for which the high-gain feedback approximation $M_{\mathrm{HG}}(s)$ is zero for all s can be determined.

Lemma 3: Consider the transfer functions in (18)–(19). The high-gain feedback approximation $M_{\mathrm{HG}}(s)$ in (7) is zero when either

$$\|\mathbf{x}_y - \mathbf{x}_u\| = \|\mathbf{x}_y - \mathbf{x}_w\| \ \wedge \ \|\mathbf{x}_z - \mathbf{x}_u\| = \|\mathbf{x}_z - \mathbf{x}_w\|, \quad (20)$$

or

$$\|\mathbf{x}_y - \mathbf{x}_u\| = \|\mathbf{x}_z - \mathbf{x}_u\| \ \wedge \ \|\mathbf{x}_y - \mathbf{x}_w\| = \|\mathbf{x}_z - \mathbf{x}_w\|. \quad (21)$$

Proof: Note that if (20) holds, it follows that $G_{yu}(s) = G_{yw}(s)$ and that $G_{zu}(s) = G_{zw}(s)$, so that (7) shows that $M_{\mathrm{HG}}(s) = 0$. Similarly, (21) implies that $G_{yu}(s) = G_{zu}(s)$ and that $G_{yw}(s) = G_{zw}(s)$, so that $M_{\mathrm{HG}}(s) = 0$. ■

To study the low-gain feedback approximation, the following asymptotic expansion of $K_0(\zeta)$ will be used

$$K_0(\zeta) \approx \sqrt{\frac{\pi}{2\zeta}} e^{-\zeta}. \quad (22)$$

The error in the approximation can be bounded by $\frac{1}{8|\zeta|}\left|\sqrt{\frac{\pi}{2\zeta}} e^{-\zeta}\right|$ when $\mathrm{Re}(\zeta) \geq 0$ (see, e.g., [20, Ch. V]). The relative error in the approximation will therefore be small for $|\zeta|$ large enough. Using this approximation, $G(s, \mathbf{x})$ in (19) can be approximated by

$$\tilde{G}(s, \mathbf{x}) = \frac{e^{-x_1 v/2D} e^{\sqrt{v^2 + 4D(h+s)}\|\mathbf{x}\|/2D}}{c_2 \sqrt{2\pi D \|\mathbf{x}\|} \sqrt[4]{v^2 + 4D(h+s)}}. \quad (23)$$

Now (18) can be approximated by

$$\begin{bmatrix} \tilde{Z}(s) \\ \tilde{Y}(s) \end{bmatrix} = \begin{bmatrix} \tilde{G}_{zw}(s) & \tilde{G}_{zu}(s) \\ \tilde{G}_{yw}(s) & \tilde{G}_{yu}(s) \end{bmatrix} \begin{bmatrix} W(s) \\ U(s) \end{bmatrix} = \begin{bmatrix} \tilde{G}(s, \mathbf{x}_z - \mathbf{x}_w) & \tilde{G}(s, \mathbf{x}_z - \mathbf{x}_u) \\ \tilde{G}(s, \mathbf{x}_y - \mathbf{x}_w) & \tilde{G}(s, \mathbf{x}_y - \mathbf{x}_u) \end{bmatrix} \begin{bmatrix} W(s) \\ U(s) \end{bmatrix}, \quad (24)$$

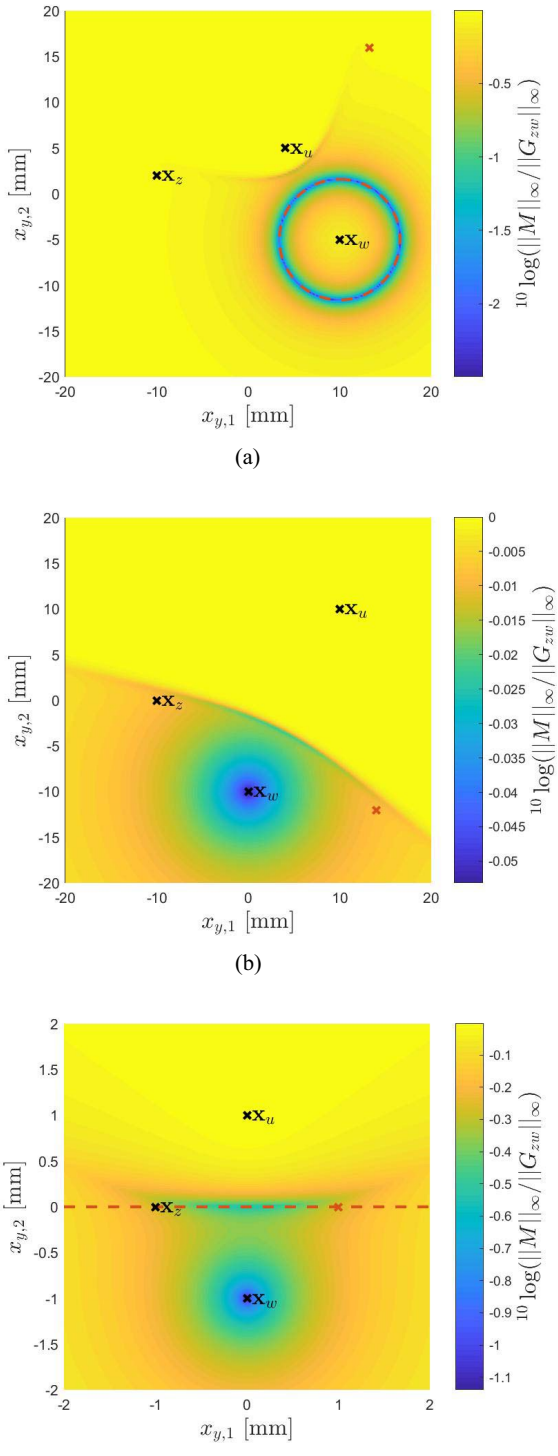

Fig. 6. Closed-loop performance $\|M\|_\infty$ for varying sensor location $\mathbf{x}_y = (x_{y,1}, x_{y,2})$ for three choices of $\mathbf{x}_z$, $\mathbf{x}_u$, $\mathbf{x}_w$ (condition (21) is satisfied at $\mathbf{x}_y = \mathbf{x}_z$ and at the red cross, condition (20) is satisfied at the dashed red line). (a) $\mathbf{x}_z = (-10, 2)$ mm, $\mathbf{x}_u = (5, 5)$ mm, $\mathbf{x}_w = (10, -5)$ mm. (b) $\mathbf{x}_z = (-10, 0)$ mm, $\mathbf{x}_u = (10, 10)$ mm, $\mathbf{x}_w = (-10, 0)$ mm. (c) $\mathbf{x}_z = (-1, 0)$ mm, $\mathbf{x}_u = (0, 1)$ mm, $\mathbf{x}_w = (0, -1)$ mm.

where $\tilde{Z}(s)$ and $\tilde{Y}(s)$ are good approximations of $Z(s)$ and $Y(s)$ when $4\sqrt{v^2 + 4Dh}\|\mathbf{x}\|/D \gg 1$.

The transfer functions in (23)–(24) can be used to find conditions under which $M_{\mathrm{LG}}(s)$ is small.

Lemma 4: Consider the transfer functions in (23)–(24). There exists a $P > 0$ such that $M_{\mathrm{LG}}(s)$ in (8) satisfies $M_{\mathrm{LG}}(0) = M'_{\mathrm{LG}}(0) = 0$ precisely when

$$\|\mathbf{x}_z - \mathbf{x}_u\| + \|\mathbf{x}_y - \mathbf{x}_w\| = \|\mathbf{x}_z - \mathbf{x}_w\| - \frac{D}{\sqrt{v^2 + 4Dh}}. \tag{25}$$

Proof: Apart from the observation that now

$$\tilde{G}'(s, \mathbf{x}) = -\left(\frac{D}{\sqrt{v^2 + 4D(h+s)}} + \|\mathbf{x}\|\right) \times \frac{\tilde{G}(s, \mathbf{x})}{\sqrt{v^2 + 4D(h+s)}}, \tag{26}$$

the proof is analogous to the proof of Lemma 2. ∎

The effectiveness of the proposed approach is validated by the numerical results in Fig. 6. These figures show the minimal value of $\|M\|_\infty$ that can be obtained for a proportional feedback controller with a modulus margin of at least 0.5 as a function of the sensor location $\mathbf{x}_y = (x_{1,y}, x_{2,y})$, where $\mathbf{x}_z$, $\mathbf{x}_w$, and $\mathbf{x}_y$ are chosen rather arbitrarily. The color scale indicates the logarithm of the reduction in closed-loop performance $\|M\|_\infty$ relative to the open-loop performance $\|G_{zw}\|_\infty$. The parameter values are $c_2 = 1150$ [J/K/m^2], $v = 0.33$ [m/s], $D = 91 \cdot 10^{-6}$ [m^2/s], and $h = 1$ [1/s].

Fig. 6(a) shows that the sensor locations where $\|M\|_\infty$ is minimal are accurately predicted by the red dashed circle around $\mathbf{x}_w$ described by (25). Note that $\|G_{yw}\|_\infty$ is negligible when $x_{1,y} > x_{1,w}$ because the problem is advection-dominated. Because $\|\mathbf{x}_z - \mathbf{x}_u\| \neq \|\mathbf{x}_z - \mathbf{x}_w\|$, (20) does not apply. Condition (21) applies when $\mathbf{x}_y = \mathbf{x}_z$ and in the location indicated by the red cross. No significant decrease in $\|M\|_\infty$ is visible at these locations, because the high-gain feedback assumption $|PG_{yu}(s)| \gg 1$ cannot be achieved.

Fig. 6(b) shows a situation where $\|\mathbf{x}_z - \mathbf{x}_w\| < \|\mathbf{x}_z - \mathbf{x}_u\|$. In this case, there are no solutions that satisfy (25). The optimal sensor location is now $\mathbf{x}_y = \mathbf{x}_w$. This is the location for which the 'mismatch' in (25) is as small as possible. Note that reduction in $\|M\|_\infty$ is significantly smaller than in Fig. 6(a). Just as in Fig. 6(a), condition (20) cannot be satisfied and no significant decrease in $\|M\|_\infty$ is observed at the locations where (21) is satisfied.

Fig. 6(c) shows again a situation where $\|\mathbf{x}_z - \mathbf{x}_w\| < \|\mathbf{x}_z - \mathbf{x}_u\|$ for which (25) cannot be satisfied. The global minimum is again at $\mathbf{x}_y = \mathbf{x}_w$. Furthermore, $\|\mathbf{x}_z - \mathbf{x}_w\| = \|\mathbf{x}_z - \mathbf{x}_u\|$ so that (20) is satisfied on the line $x_{y,2} = 0$. Indeed, $\|M\|_\infty$ decreases on this line, especially at locations $\mathbf{x}_y$ near $\mathbf{x}_u$ at which the high-gain feedback assumption $|PG_{yu}(s)| \gg 1$ can be approximated better.

IV. Conclusion and Future Work

A proportional feedback control system design problem for one- and two-dimensional advection-diffusion equations with constant coefficients has been studied. Simple geometric rules have been derived describing the sensor and actuator locations for which high-gain and low-gain proportional feedback control can best reduce the influence a disturbance applied at a given point. The derivation is based on high-gain and low-gain approximations of the analytic expression for the closed-loop transfer function. Numerical experiments indicate that the rules predict all locally optimal locations.

On the 1-D spatial domain, there are either one, two, or three locally optimal sensor or actuator locations depending on the ordering of the other input and output locations. The three possible orderings of the other input and output locations are shown in Fig. 2. The optimal locations are accurately predicted by the conditions in Lemma 1 and 2. On the 2-D spatial domain, the locally optimal sensor locations are mainly characterized by Lemma 4.

For the wafer heating problem in [18] it would be interesting to extend the results to thermomechanical systems in which the performance variable $z(t)$ does not represent the temperature, but the displacement. Furthermore, extensions to spatially distributed inputs, noisy measurements, and dynamic feedback controllers are interesting topics for future research.

References

[1] M. van de Wal and B. de Jager, "A review of methods for input/output selection," *Automatica*, vol. 37, no. 4, pp. 487–510, 2001.

[2] J. A. Burns and D. Rubio, "A distributed parameter control approach to sensor location for optimal feedback control of thermal processes," in *Proc. CDC*, 1997, pp. 2243–2247.

[3] J. A. Burns and C. N. Rautenberg, "Solutions and approximations to the Riccati integral equation with values in a space of compact operators," *SIAM J. Control Optim.*, vol. 53, no. 5, pp. 2846–2877, 2015.

[4] J. A. Burns and C. N. Rautenberg, "The infinite-dimensional optimal filtering problem with mobile and stationary sensor networks," *Numer. Funct. Anal. Optim.*, vol. 36, no. 2, pp. 181–224, 2015.

[5] A. Armaou and M. A. Demetriou, "Using spatial $\mathcal{H}_2$ norm for sensor placement in parabolic partial differential equations," in *Proc. ACC*, 2006, pp. 1467–1472.

[6] U. Vaidya, R. Rajaram, and S. Dasgupta, "Actuator and sensor placement in linear advection PDE," in *Proc. CDC*, 2011, pp. 5395–5400.

[7] Y. Privat, E. Trélat, and E. Zuazua, "Optimal shape and location of sensors for parabolic equations with random initial data," *Archive Ration. Mech. Anal.*, vol. 216, no. 3, pp. 921–981, 2015.

[8] Y. Privat, E. Trélat, and E. Zuazua, "Actuator design for parabolic distributed parameter systems with the moment method," *SIAM J. Control Optim.*, vol. 55, no. 2, pp. 1128–1152, 2017.

[9] K. Morris, "Linear-quadratic optimal actuator location," *IEEE Trans. Autom. Control*, vol. 56, no. 1, pp. 113–124, Jan. 2011.

[10] N. Darivandi, K. Morris, and A. Khajepour, "An algorithm for LQ optimal actuator location," *Smart Mater. Struct.*, vol. 22, no. 3, 2013, Art. no. 035001.

[11] D. Kasinathan and K. Morris, "$\mathcal{H}_\infty$-optimal actuator location," *IEEE Trans. Autom. Control*, vol. 58, no. 10, pp. 2522–2535, Oct. 2013.

[12] K. K. Chen and C. W. Rowley, "$\mathcal{H}_2$ optimal actuator and sensor placement in the linearised complex Ginzburg–Landau system," *J. Fluid Mech.*, vol. 681, pp. 241–260, Aug. 2011.

[13] M. Zhang and K. Morris, "Sensor choice for minimum error variance estimation," *IEEE Trans. Autom. Control*, vol. 63, no. 2, pp. 315–330, Feb. 2018.

[14] M. A. Demetriou, "Robust sensor location optimization in distributed parameter systems using functional observers," in *Proc. CDC*, 2005, pp. 7187–7192.

[15] M. A. Demetriou, "Sensor selection and static output feedback of parabolic PDEs via state feedback kernel partitioning using modification of Voronoi tessellations," in *Proc. ACC*, 2017, pp. 2497–2503.

[16] R. F. Curtain and K. Morris, "Transfer functions of distributed parameter systems: A tutorial," *Automatica*, vol. 45, no. 5, pp. 1101–1116, 2009.

[17] K. A. Morris, "Noise reduction in ducts achievable by point control," *J. Dyn. Syst. Meas. Control*, vol. 120, no. 2, pp. 216–223, 1998.

[18] D. W. M. Veldman, R. H. B. Fey, H. J. Zwart, M. M. J. van de Wal, J. D. B. J. van den Boom, and H. Nijmeijer, "Semi-analytic approximation of the temperature field resulting from moving heat loads," *Int. J. Heat Mass Transf.*, vol. 122, pp. 128–137, Jul. 2018.

[19] D. W. Hahn and M. N. Özişik, *Heat Conduction*. Hoboken, NJ, USA: Wiley, 2012.

[20] A. Gray and G. B. Mathews, *A Treatise on Bessel Functions and Their Applications to Physics*, 2nd ed. London, U.K.: Macmillan, 1952.